Computers in Physics

More on Fractals and Chaos: Multifractals

Harvey Gould and Jan Tobochnik

Citation: Computers in Physics **4**, 202 (1990); doi: 10.1063/1.4822901
View online: http://dx.doi.org/10.1063/1.4822901
View Table of Contents: http://scitation.aip.org/content/aip/journal/cip/4/2?ver=pdfcov
Published by the AIP Publishing

COMPUTER SIMULATIONS

More On Fractals And Chaos: Multifractals

Harvey Gould and Jan Tobochnik

In recent columns we and our contributors have discussed various aspects of fractals and chaos. Family and Vicsek[1] discussed ways of obtaining complex geometrical objects from simple aggregation processes and we showed that the trajectories of chaotic systems are fractal objects called strange attractors.[2] In this issue we discuss multifractals in more detail and some of the connections between fractals and chaos.

We know that a fractal object[3–9] can be characterized by the fractal dimension, a measure of how the density of the object varies with length scale. However, there are more complicated objects known as *multifractals* for which it is now recognized that it is necessary to define a continuous spectrum of dimensions to characterize them.[6–8] Why might we need more than the fractal dimension to characterize some objects? One answer is that two objects with the same fractal dimension can be quite different visually.

Before we learn how to characterize multifractals, we first consider simple fractal objects that can be described by only the fractal dimension. In Fig. 1 we show a straight line segment of unit length that is covered by N pieces each of size ℓ. The fractal dimension d_f of an object can be obtained from the relation

$$N \sim \ell^{-d_f} \quad (\ell \ll 1). \tag{1}$$

For a line segment we know that $N = 1/\ell$ and hence $d_f = 1$. If we draw a square on a piece of paper and divide it into small squares of linear dimension ℓ, then $N = 1/\ell^2$, and $d_f = 2$. That is, for a nonfractal object $d_f = d$, where d is the spatial dimension, and the dimension of the covering object equals the dimension of the space in which the object is embedded.

Now consider a (triadic) Koch curve whose two ends are at 0 and 1 (see Fig. 2). At each stage of the construction of this curve, the number of straight line segments increases by 4 and the size of each segment decreases by $\frac{1}{3}$. We can associate ℓ with the size of a line segment and we see from Fig. 2 that after k iterations, $N = 4^k$, and $\ell = (1/3)^k$. In order to find the fractal dimension of the Koch curve, we substitute these relations for N and ℓ into (1) and we find that $d_f = \ln 4/\ln 3 \approx 1.26$ with $d_f \neq d$. Note that if we associate a uniform mass density with the Koch curve, the mass of each line segment at the kth iteration is identical. It is this feature that allows the geometrical structure of the Koch curve and other simple fractals to be characterized by a single scaling exponent. This feature is not shared by multifractals, where the mass enclosed by d-dimensional boxes of volume ℓ^d depends on the location of the boxes on the fractal.

In order to introduce the idea of multifractals, we generate a multifractal using a nonuniform generalization of the Koch curve. At the kth iteration we divide each segment into four segments as before, but now we distribute the mass so that two segments receive a fraction p_1 and the other two receive a fraction p_2, such that $2p_1 + 2p_2 = 1$. The division distributes the mass of the object among the line segments nonuniformly and thus the linear mass density along the Koch curve varies. If we assign unit mass to the original curve, then for $k = 1$, two of the line segments have mass p_1 and two segments have mass p_2. For $k = 2$ there are 16 segments, four with mass p_1^2, four with mass p_2^2, and eight with mass $p_1 p_2$. For $k = 3$, there is even more variation in the masses of the line segments. Each set of segments with the same mass constitutes a fractal and the entire collection is a multifractal.

In order to describe this fractal object, we need to know how the mass p_w of segment type w and N_w, the number of segments of segment type w, scales with segment size ℓ. We write

$$p_w(\ell) \sim \ell^{\alpha_w}, \tag{2}$$

$$N_w(\ell) \sim \ell^{-f_w}, \tag{3}$$

where we have introduced the exponents α_w and f_w and $w = 0, 1, \ldots k$. The mass of type w and k iterations is $p_w = p_1^w p_2^{k-w}$, where the index w determines a particular subfractal in which each segment has the same mass.

A plot of f versus α is referred to as the f–α spectrum and is the usual plot associated with a multifractal analysis. In this simple example we can compute the f–α spectrum analytically by solving (2) for α_w using the relationship $p_w = p_1^w p_2^{k-w}$ and $\ell = (1/3)^k$. The result is

$$\alpha_w = [w \ln p_1 + (k-w) \ln p_2]/k \ln(1/3). \tag{4}$$

Since the number of segments of mass p_w at the kth

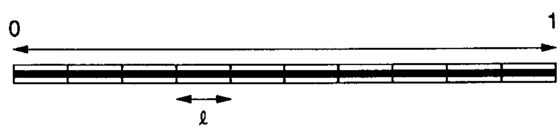

Fig. 1. A straight line segment covered by $N = 10$ objects of dimension ℓ.

Harvey Gould is professor of physics at Clark University, Worcester, MA 01610. Jan Tobochnik is assistant professor of physics and computer science at Kalamazoo College, Kalamazoo, MI 49007.

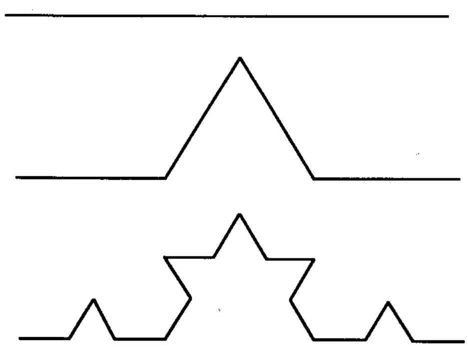

Fig. 2. The first three iterations of the triadic Koch curve.

iteration is $N_w = 2^k\binom{k}{w}$, where $\binom{k}{w}$ is the binomial coefficient, we obtain from (3) that

$$f_w = -\ln 2^k k!/(k-w)!w!/k\ln(1/3).$$

We can then use Stirling's approximation to find

$$f_w = -[k\ln k - (k-w)\ln(k-w) - w\ln w + k\ln 2] \times [k\ln(1/3)]^{-1}. \quad (5)$$

A plot of f_w vs α_w for $p_1 = \frac{1}{6}$ is shown in Fig. 3.

In the Koch curve example, the mass associated with each segment was imposed in an *ad hoc* manner. We now extend the multifractal analysis to the case where the fractal is produced by a statistical process, e.g., diffusion-limited aggregation, or by the strange attractor of a dynamical system. We will find that these fractals can be described by a continuously varying spectrum of fractal dimensions, i.e., we can think of each fractal as made of an infinite collection of fractals each with its own fractal dimension. We emphasize that the multifractal analysis can be applied to any probability distribution, e.g., the distribution of voltages drops in a random resistor network, and not only to the distribution of mass.

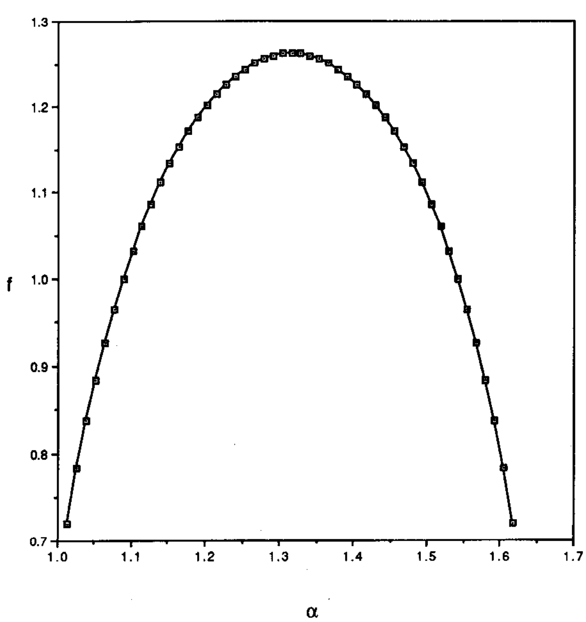

Fig. 3. The f–α spectrum for a nonuniform Koch curve with $p_1 = \frac{1}{6}$. Note that the maximum value of f is $\ln 4/\ln 3 \approx 1.26$, the fractal dimension.

Just as a list of the positions and momenta of the particles in a liquid is not very useful, a list of the positions of the occupied sites in a geometrical fractal is also not very useful. The most complete statistical description of a fractal object would be the fraction of the total mass of the object enclosed in a region $d\mathbf{r}$ centered about the position $\mathbf{r}$. Since most calculations are done numerically, the simplest choice for the volume element $d\mathbf{r}$ is a d-dimensional box of linear dimension ℓ. The position of the boxes is given by the index i and the corresponding probability is denoted as $p_i(\ell)$. Usually the probability provides too much information and we are more interested in averages over p_i. The mathematical quantity analogous to the partition function in statistical mechanics is the sum over all boxes of the qth power of the probabilities:

$$\chi_0(\ell) \equiv \sum_i p_i^q(\ell), \quad (6)$$

where the sum is over all boxes and $-\infty < q < \infty$. The quantity q is analogous to the temperature in statistical mechanics. Note that

$$\chi_1 = \sum_i p_i = 1$$

as is required for a normalized probability, and that χ_1 is independent of ℓ.

The quantity ℓ in (6) sets the length scale for the probability distribution. Since we are interested in the scaling properties of the fractal, we want to know how χ_q scales with ℓ for a continuous range of q values. We expect that

$$\chi_q(\ell) \sim \ell^{(q-1)D_q}, \quad (7)$$

where D_q is known as the *generalized dimension of order q*. The factor of $q-1$ appears in (7) so that χ_1 is independent of ℓ. The relation $D_0 = d_f$ follows from the ℓ dependence of χ_0 since the latter measures the number of boxes that contain a part of the fractal. In the simple case of uniform fractals, $D_q = D_0$ for all q.

The small ℓ scaling dependence of χ_q expressed by (7) can be divided into two parts. For each q there are certain boxes that make the dominant contribution to χ_q in the limit $\ell \to 0$. This subset of boxes forms a fractal with a fractal dimension f_q that depends on q. We write

$$N_q(\ell) \sim \ell^{-f_q}, \quad (8)$$

where $N_q(\ell)$ is the number of boxes that give the domiant contribution in (6). These boxes have the same probability p_q corresponding to one of the subfractals already mentioned. The dependence of $p_q(\ell)$ on ℓ can be expressed as

$$p_q(\ell) \sim \ell^{\alpha_q}. \quad (9)$$

The quantity of main interest is the dependence of f_q on α_q. Large α corresponds to parts of the fractal that are very ramified, and small α corresponds to parts that are less ramified. If there is a part where $\alpha = d$, this part has a uniform density corresponding to a nonfractal object. An object with a single value of $\alpha = d_f$ is a monofractal.

How do we compute f_q vs α_q? First we note that by putting together the two relations (8) and (9) that comprise the small ℓ dependence of χ_q given by (7), we arrive at the relation

$$(q-1)D_q = q\alpha_q - f_q. \tag{10}$$

D_q can be extracted from (7) by computing $\chi_q(\ell)$ using (6). In order to compute α_q, we treat α as an independent continuous variable and calculate χ by integrating over α:

$$\chi_q = \int \ell^{q\alpha' - f(\alpha')}\, d\alpha'. \tag{11}$$

The dominant contribution to the integral in (11) arises from the value of α for which the exponent of ℓ is an extremum, i.e., at $\alpha = \alpha_q$, the quantity of interest. We find that

$$\left.\frac{df(\alpha)}{d\alpha}\right|_{\alpha=\alpha_q} = q. \tag{12}$$

We use (12) and the result

$$\frac{d(q\alpha_q - f_q)}{dq} = \alpha_q + q\frac{d\alpha_q}{dq} - \frac{df_q}{d\alpha_q}\frac{d\alpha_q}{dq} = \alpha_q$$

to obtain

$$\alpha_q = \frac{d}{dq}[(q-1)D_q]. \tag{13}$$

We use the above relations to summarize the procedure for computing the f–α spectrum as follows:

1. Compute χ_q using the definition (6) for different values of ℓ. Extract D_q from these data using the definition (7).

2. Calculate α_q from (13) by numerically differentiating $(q-1)D_q$ with respect to q.

3. Use (10) and the results for D_q and α_q to find f_q. Plot f_q vs α_q.

For a deterministic chaotic system the computation of p_i is straightforward. We divide space into boxes of linear dimension ℓ, iterate the equations of motion (differential equations or difference equations), and then count the number of times the trajectory lies in each box. In Fig. 4 we show the f–α spectrum computed according to this procedure for the logistic map at the accumulation point $r = r_c \approx 0.8925$.

For diffusion-limited aggregation, we can identify p_i with the growth probability that the next random walker will land at a surface site labeled by the index i. In order to determine p_i, it is necessary to solve Laplace's equation numerically.[10] The distribution of the probabilities is illustrated in Fig. 3 of the previous column[1] by assigning different colors to the perimeter sites. Recently Vicsek *et al.*[11] have shown that the mass distribution in DLA also exhibits multifractal scaling (see Problem 6).

The multifractal analysis that we have discussed is very general and can be used for any probability distribution such as the distribution of galaxies in the sky.[12] Several examples including an application to random resistor networks are discussed in Ref. 6. At present the main value of the multifractal analysis is to characterize the nature of probability distribution generated either in a laboratory experiment or by a computer simulation. In order for a true understanding of fractals

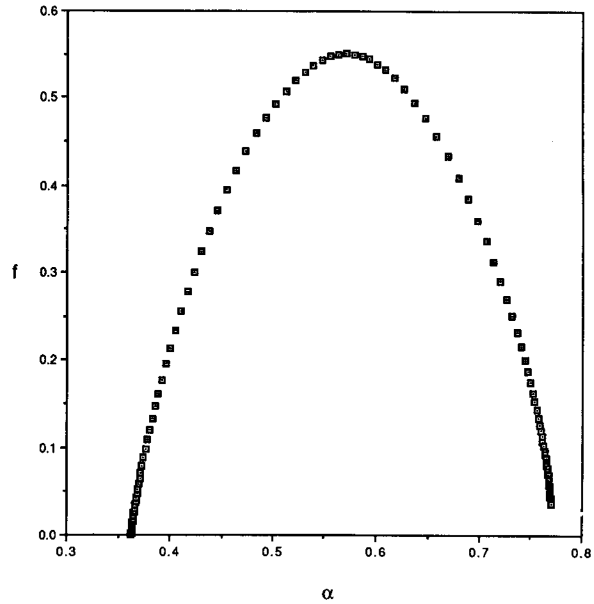

Fig. 4. The f–α spectrum for the logistic map at $r = r_c \approx 0.8925$. The probabilities p_i were computed after 10 000 iterations with box sizes ℓ given by $\ell = 0.5^n$ with $n = 1,\ldots,10$. The moments χ_q were computed for $-20 \leqslant q \leqslant 20$ in intervals of $\Delta q = 0.2$.

and chaos to emerge, we need to know not only how to measure the multifractal spectrum, but how a particular multifractal spectrum arises from the mechanisms that generate the fractal. That is, we need the tools equivalent to perturbation theory, mean field theory, renormalization group techniques, etc., that are well developed in equilibrium statistical mechanics. We still have a long way to go toward understanding the why of multifractals.

Suggestions for Further Study

1. Use the exact relations (4) and (5) to plot the f–α spectrum of the nonuniform Koch curve for various values of p_1. Choose $k = 100$ and find f and α with w running from 1 to k. Begin with $p_1 = \frac{1}{8}$ and increase p_1 in increments of 0.025. How sensitive are your results to the value of k? What happens to the f–α spectrum as p_1 approaches $\frac{1}{4}$? Also plot f and α as functions of w to obtain a sense of the width of their distribution. How would (4) and (5) be changed if the size of the line segments varied nonuniformly in addition to the probabilities? How would you extend the analysis if each of the four segments had different probabilities at each iteration? Think of other extensions to the nonuniform Koch curve.

2. The *information dimension* $D_{\rm inf}$ can be defined as

$$D_{\rm inf} = -\lim_{l\to 0} S(\ell)/\ln \ell, \tag{14}$$

where

$$S(\ell) = -\sum_i p_i \ln p_i. \tag{15}$$

Show that the dimension D_1 defined as [see (6) and (7)]

$$D_1 = \lim_{\ell\to 0}\lim_{q\to 1}\frac{1}{(q-1)}\frac{\ln \Sigma p_i^q}{\ln \ell} \tag{16}$$

is equivalent to $D_{\rm inf}$.

3. Use the procedure outlined in the text to find the f–α spectrum for the logistic map $x_{n+1} = 4rx_n(1-x_n)$, for various values of r. The system becomes chaotic above $r \gtrsim 0.8925$. Plot f_q, α_q, and D_q as functions of q. Consider on the order of 10 000 iterations or more and q in $-20 \leqslant q \leqslant 20$ in intervals of $\Delta q = 0.2$. It is straightforward to extend the multifractal analysis to the strange attractor of the two-dimensional Henon map. (See, for example, the discussion of the Henon map in Ref. 2.)

4. The method discussed in the text for determining p_i is known as *box counting*. In this method the fractal is covered with a grid of boxes of volume ℓ^d and the limit $l \to 0$ is considered. If the fractal can grow indefinitely, we can fix the box dimension at ℓ, where ℓ is sufficiently large to contain a number of lattice sites, but much smaller than L, the linear dimension of the fractal. We can then determine p_i as a function of ℓ/L for larger and larger L. However, in order to satisfy the condition $\ell \ll L$, extremely large fractals must be considered. If we are interested in the distribution of mass, the *sandbox method* in which the number of points $M(R)$ within a region of radius R is counted yields better results than the box counting method. If the centers of the boxes are centered randomly on the fractal, we can assume that

$$\left\langle \left(\frac{M(R)}{M_0}\right)^{q-1}\right\rangle \sim \left(\frac{R}{L}\right)^{(q-1)D_q}, \qquad (17)$$

where M_0 is the total mass of the fractal and $\langle \cdots \rangle$ denotes an average over the centers of the boxes. Suppose that 500 000 particles (with zero linear dimension) are randomly distributed in a two-dimensional box with $L = 3000$. What would you expect to find for the generalized dimensions D_q? Use the sandbox method to compute D_q for randomly distributed particles in a one-dimensional box.

5. Consider a random walk in $d = 1$ for which a walker takes random unit steps on a lattice with unit lattice spacing. At each step the walker drops a bread crumb of mass unity. Perform a multifractal analysis of the mass distribution. Is the mass distribution a multifractal?

6. As mentioned in the text, the computation of the f–α spectrum for the mas distribution of DLA is nontrivial and very large clusters must be used to obtain reasonable results for the spectrum.[10] (Small clusters appear to yield a spectrum consistent with a simple fractal.) The difficulties associated with measuring the moments of a multifractal distribution are emphasized in Ref. 13. A problem of current interest is the multifractal spectrum of percolation clusters.[14] Although it is likely that percolation clusters are simple monofractals, their multifractal behavior is not known. Generate large single clusters at $p = p_c$ in two dimensions using the algorithm due to Hammersley, Leath, and Alexandrowicz.[15] Use the sandbox method and perform a multifractal analysis. Do your numerical results convince you that percolation clusters are simple fractals?

Please send us your results and comments for further columns. Graphically oriented programs relevant to the suggested problems are available from the authors in True BASIC for IBM PC compatibles and Macintosh computers. Please address comments and requests to hgould@clarku or tobochnik@heyl.kzoo.edu.

Acknowledgment

We thank Fereydoon Family for useful suggestions.

References

1. F. Family and T. Vicsek, Comput. Phys. **4**(1), 44 (1990).
2. J. Tobochnik and H. Gould, Comput. Phys. **3**(5), 86 (1989).
3. B. B. Mandelbrot, *The Fractal Geometry of Nature* (Freeman, San Francisco, 1982).
4. J. Feder, *Fractals* (Plenum, New York, 1988).
5. T. Vicsek, *Fractal Growth Phenomena* (World Scientific, Singapore, 1989).
6. G. Paladin and A. Vulpiani, Phys. Rep. **156**, 148 (1987).
7. H. G. E. Hentschel and I. Procaccia, Physica D **8**, 435 (1983).
8. T. C. Halsey, M. H. Jensen, L. P. Kadanoff, I. Procaccia, and B. I. Shraiman, Phys. Rev. A **33**, 1141 (1986).
9. H. E. Stanley and P. Meakin, Nature **335**, 405 (1988).
10. P. Meakin, "The growth of fractal aggregates and their fractal measures," in *Phase Transitions and Critical Phenomena*, edited by C. Domb and J. L. Lebowitz (Academic, New York, 1988).
11. T. Vicsek, F. Family, and P. Meakin, preprint (1990).
12. H. Atmanspacher, H. Scheingraber, and G. Wiedenmann, Phys. Rev. A **40**, 3954 (1989).
13. A. Aharony, Physica D **38**, 1 (1989).
14. F. Family (private communication).
15. See, for example, H. Gould and J. Tobochnik, *Introduction to Computer Simulations* (Addison-Wesley, Reading, MA, 1988), Chap. 13.